



HAL
open science

Aluminum, oxide and silicon phonons by IETS on MOS tunnel junctions : accurate determination and effect of electrical stress

C. Petit, G. Salace, D. Vuillaume

► **To cite this version:**

C. Petit, G. Salace, D. Vuillaume. Aluminum, oxide and silicon phonons by IETS on MOS tunnel junctions : accurate determination and effect of electrical stress. *Journal of Applied Physics*, 2004, 96, pp.5042-5049. hal-00140733

HAL Id: hal-00140733

<https://hal.science/hal-00140733>

Submitted on 25 May 2022

HAL is a multi-disciplinary open access archive for the deposit and dissemination of scientific research documents, whether they are published or not. The documents may come from teaching and research institutions in France or abroad, or from public or private research centers.

L'archive ouverte pluridisciplinaire **HAL**, est destinée au dépôt et à la diffusion de documents scientifiques de niveau recherche, publiés ou non, émanant des établissements d'enseignement et de recherche français ou étrangers, des laboratoires publics ou privés.

Aluminum, oxide, and silicon phonons by inelastic electron tunneling spectroscopy on metal-oxide-semiconductor tunnel junctions: Accurate determination and effect of electrical stress

Cite as: J. Appl. Phys. **96**, 5042 (2004); <https://doi.org/10.1063/1.1775299>

Submitted: 01 March 2004 • Accepted: 02 June 2004 • Published Online: 28 October 2004

C. Petit, G. Salace and D. Vuillaume



View Online



Export Citation

ARTICLES YOU MAY BE INTERESTED IN

[Quantitative inelastic tunneling spectroscopy in the silicon metal-oxide-semiconductor system](#)

Applied Physics Letters **71**, 2523 (1997); <https://doi.org/10.1063/1.120106>

[Generalized Formula for the Electric Tunnel Effect between Similar Electrodes Separated by a Thin Insulating Film](#)

Journal of Applied Physics **34**, 1793 (1963); <https://doi.org/10.1063/1.1702682>

[Inelastic electron tunneling spectroscopy: Capabilities and limitations in metal-oxide-semiconductor devices](#)

Journal of Applied Physics **91**, 5896 (2002); <https://doi.org/10.1063/1.1462423>

Lock-in Amplifiers
up to 600 MHz



Zurich
Instruments



Aluminum, oxide, and silicon phonons by inelastic electron tunneling spectroscopy on metal-oxide-semiconductor tunnel junctions: Accurate determination and effect of electrical stress

C. Petit^{a)}

Dynamique de Transfert aux Interfaces, DTI, UMR CNRS 6107, Université de Reims, Boîte Postale 1039, 51687 Reims Cedex 2, France and Laboratoire d'Automatisme et de Microélectronique, LAM, Université de Reims, Boîte Postale 1039, 51687 Reims Cedex 2, France

G. Salace

Dynamique de Transfert aux Interfaces, DTI, UMR CNRS 6107, Université de Reims, Boîte Postale 1039, 51687 Reims Cedex 2, France

D. Vuillaume

Institut d'Electronique, de Microélectronique, et de Nanotechnologie, IEMN, UMR CNRS 8520, avenue Poincaré, Boîte Postale 69, 59652 Villeneuve d'Ascq Cedex, France

(Received 1 March 2004; accepted 2 June 2004)

We do inelastic electrical tunneling spectroscopy (IETS) to provide information concerning the vibrational and excitational modes present in silicon dioxide and phonon modes of the electrodes, and of silicon dioxide in metal-oxide-silicon tunnel junction. We analyze the phonon spectra coming from different parts of the metal-oxide-semiconductor (MOS) junction: the aluminum gate, the SiO₂ ultrathin film, and the silicon substrate. We compare the phonon modes for the (100) and (111) silicon orientations. We show that IETS can reveal the modifications of Si-SiO₂ interface induced by electrical stresses. After a constant voltage stress, the silicon longitudinal phonon modes are significantly shifted in energy, while the transversal phonon modes stay unaffected. Interface healing after annealing is also observed by IETS. These features make IETS a useful tool for MOS reliability studies. © 2004 American Institute of Physics. [DOI: 10.1063/1.1775299]

I. INTRODUCTION

Tunneling transport plays a crucial role in ultrathin oxide device, and the trap-assisted inelastic is often proposed as a conduction mechanism of stress induced leakage current damage.¹⁻³ The tunneling electrons can interact with molecular vibrations in the insulator and also with lattice vibrations of the three parts (silicon, oxide, and gate electrode) of the metal-oxide-semiconductor (MOS) device. In the inelastic electron tunneling spectroscopy (IETS) technique, these interactions are detected as peaks in the second derivative of current-voltage characteristics at low temperature (4.2 K). Thirty years ago, IETS was used to probe the chemisorption of organic molecules on thin amorphous films of Al₂O₃ (Ref. 4) and other insulators.⁵ There has been much work applying this technique to metal-insulator-metal (MIM) junctions⁶⁻¹⁰ since the first pioneering paper.¹¹ More recently, IETS was employed to investigate Langmuir-Blodgett monolayers¹²⁻¹⁴ and for the direct observation of magnon excitations.^{15,16} The first application of the IETS technique to MOS devices was made by Bencuya.¹⁷ Then, other authors have demonstrated the application of tunneling spectroscopy to the silicon MOS system.¹⁸⁻²¹ In a previous paper, we reported several results about IETS on MOS devices in an extended energy range up to 350 mV (2823 cm⁻¹).²² We demonstrated that this technique may be an interesting diagnostic method for the characterization of the most recent manufactured MOS devices

with ultrathin oxides. In this paper, we focus on the identification of phonon modes of both electrodes, silicon substrate and Al gate, in Al-SiO₂-Si (*n*⁺ or *p*⁺) structures. The (100) silicon substrate orientation is compared to the previously reported (111) orientation.²² Phonon spectra of tunnel SiO₂ barrier grown on (111) and (100) silicon are reported and compared with literature data. The energy level locations of the deconvoluted IETS peaks are discussed and compared to assignments reported in the well-established literature. We report for the (100) orientation, the most interesting in microelectronics, an amazing and interesting change in the lattice vibration spectra of the silicon phonon mode peaks after the application of electrical stresses. We discuss these modifications as regard of these electrical stresses.

II. SAMPLE PREPARATION AND IETS MEASUREMENTS

Al-SiO₂-Si (*n*⁺ or *p*⁺) capacitors were fabricated at the Institut d'Electronique, de Microtechnologie et de Nanotechnologie (IEMN) on highly doped silicon samples (*N*_A or *N*_D in the range of 1.3 × 10¹⁸–4.7 × 10¹⁹ cm⁻³ with, respectively, boron and phosphorous impurities). The wafers were provided by Siltronic Company. Both the (100) and (111) orientations have been chosen for reason of comparison. Ultrathin silicon oxide films were grown by thermal oxidation in dry O₂ at 600 °C for 4 min (oxide thickness 2.1 nm as measured by ellipsometry) followed by a postoxidation anneal in dry N₂ at 600 °C for 30 min in the same oven. After thermal oxidation, aluminum gates were deposited (thickness

^{a)}FAX: (333) 26.91.33.12; electronic mail: christian.petit@univ-reims.fr

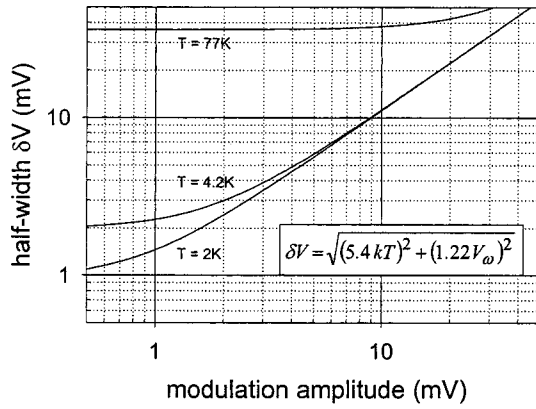


FIG. 1. Full width half-maximum vs voltage modulation for the temperature values 2, 4.2, and 77 K.

300 nm) by e^- -beam evaporation (using an electron gun in a 10^{-8} torr vacuum chamber) through shadow masks to define square electrodes with areas of 1×10^{-2} and 3.6×10^{-3} cm².

The inelastic electron tunneling (IET) spectra were obtained by the modulation technique using a lock-in amplifier. The experimental set up was described in a previous paper.²³ The resistance of tunnel junctions are in the range of 100–500 Ω corresponding to a well-adapted impedance in our derivative setting. By pumping the cryostat, above the helium liquid phase, it is possible to lower the bath temperature from 4.2 K down to 1.9 K. This improves the spectra resolution. The effects of temperature T and modulation voltage amplitude V_ω on the peak width, intensity, and line shape were studied. If we consider only these two parameters, the full width at half maximum (FWHM) on the line peak is given by

$$\delta V = \sqrt{(5.4kT)^2 + (1.22eV_\omega)^2},$$

where k is the Boltzmann constant and e the electron charge.

In Fig. 1, we plot the FWHM versus the modulation voltage for three measured temperatures, and in Fig. 2 we

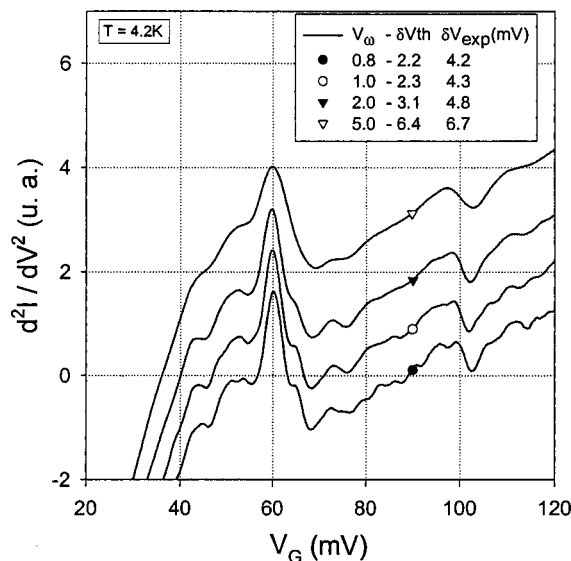


FIG. 2. IET spectra for the modulation voltage values 0.8, 1, 2, and 5 mV at the temperature $T=4.2$ K for an Al-SiO₂-Si (n^+) junction.

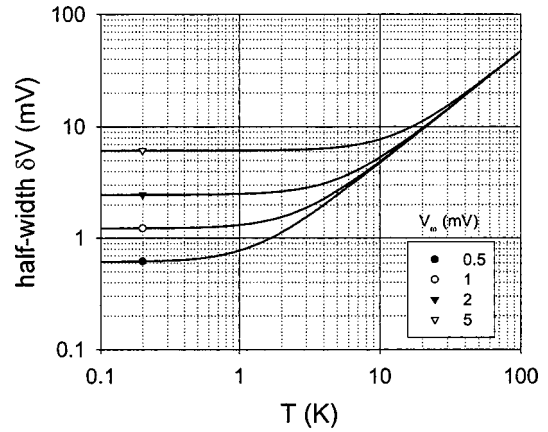


FIG. 3. Full width half-maximum vs temperature for voltage modulation values 0.5, 1, 2, and 5 mV.

show a typical IETS spectrum [sample Al-SiO₂-Si (n^+) of IEMN] for four amplitude modulations. In the insert, we give the experimental and calculated FWHM δV . We can observe an improvement of the FWHM δV when the amplitude modulation decreases. Shen and Li²⁴ demonstrated that the optimum measurement condition for a good detection of IETS peaks is about $kT/eV_\omega=0.2$. At 4.2 K (liquid helium temperature), the optimum measurement involves a modulation amplitude of 1.6 mV. In Fig. 3, we plot the FWHM versus temperature for four voltage modulations and, in Fig. 4, the IET spectrum curve for the same sample as in Fig. 2 and at two temperatures. The δV resolution decreases when the sample temperature is lowered, but if T is very small, a drop in temperature T produces insignificant decreases in width δV . At $V_\omega=0.8$ mV, the optimum condition involves a temperature of 1.85 K. In the insert of Fig. 4, we show the experimental and calculated FWHM δV . These experimental values are obtained after subtraction of background and

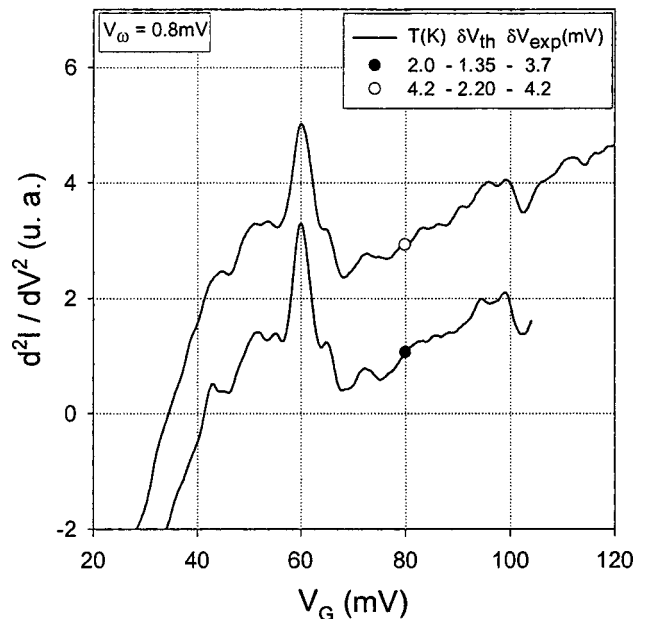


FIG. 4. IET spectra for the modulation voltage value 0.8 at the temperature values 2 and 4.2 K for an Al-Si O₂-Si (n^+) junction.

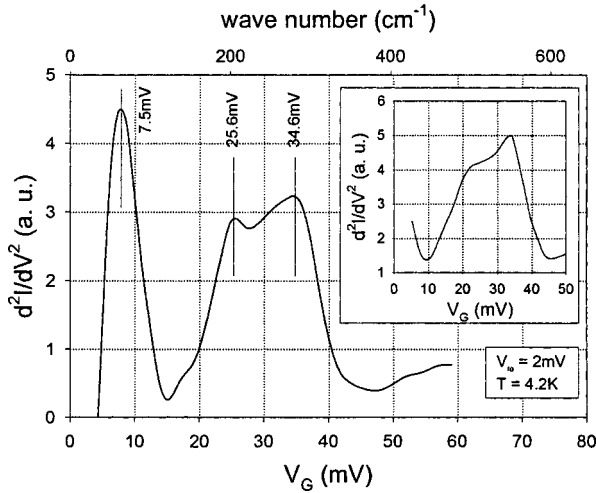


FIG. 5. Aluminum phonons spectra Al-SiO₂-Si (*p*⁺) (100) at low energy. In the insert, IET spectrum obtained by Klein with an Al-Al₂O₃-Al tunneling junction (see Ref. 28).

peak deconvolution. We can note the difference between the experimental and theoretical FWHM: the experimental lines are much broader. Wamsley *et al.*²⁵ explained this difference by attributing a natural width δV_{nat} to the vibration mode peak with a Gaussian profile. In our opinion, this intrinsic line width is partly due to the difficulty to determine the accurate background of the line, and partly due to the natural peak line width resulting from the inelastic tunneling interaction with the vibration modes.^{26,27} With this new parameter δV_{nat} , the full width at half maximum of the peak is given by

$$\delta V = \sqrt{(5.4kT)^2 + (1.22eV_\omega)^2 + (\delta V_{nat})^2}.$$

In our experiments, we have found δV_{nat} of about 2 mV. Wamsley *et al.*²⁵ have given a corresponding value of 1.504 mV, while recently Lauhon and Ho²⁷ have reported an intrinsic width of 4 ± 2 mV on single molecule vibrational spectroscopy with scanning tunneling microscope. But, as outlined by Bencuya,¹⁷ usually the V_ω modulation voltage is more serious limitation than the temperature one.

III. PHONONS OF THE ELECTRODES

A. Phonons of the aluminum gate

In Fig. 5, we show an IET spectrum of an Al-SiO₂-Si (*p*⁺) (100) tunneling junction. This second derivative of the *I-V* characteristics has been obtained at liquid helium temperature (*T*=4.2 K) with a modulation magnitude of 2 mV (4 mV peak to peak). A strong structure appears in the low voltage region from 20 to 40 meV. This corresponds to a large relative conductance change in the first derivative (about 12%). The 0–50 meV region of Fig. 5 is compared with the Al-Al₂O₃-Al spectrum obtained by Klein (see the insert).²⁸ This last spectrum was observed by Klein and Leger²⁹ and attributed to phonon structure in granular aluminum. Two peaks (25.6 meV, 34.6 meV), superimposed on a general background, were attributed to acoustical phonons (transverse, longitudinal) in the aluminum by these authors. The peak positions in our case are very close (25.6 meV, 34.6 meV) and they are in good agreement with

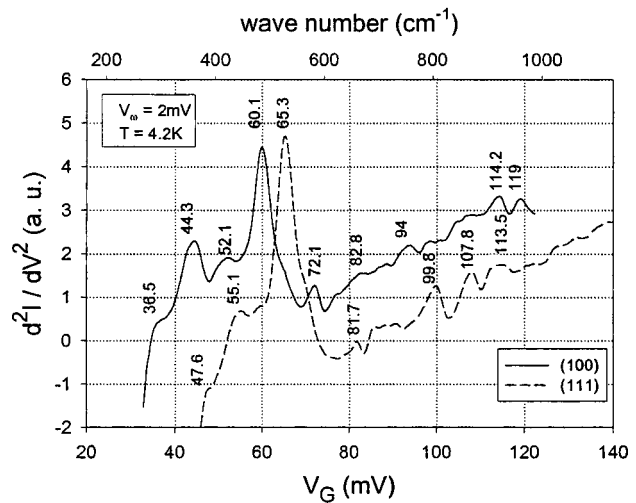


FIG. 6. Silicon phonons spectrum of an Al-SiO₂-Si (*n*⁺) junction for (100) and (111) silicon orientation.

the phonon spectrum for bulk Al as deduced from neutron scattering.³⁰ The peak at 7.5 meV is due to a zero bias anomaly.

Now, let us consider the conductance change both in the MIM and MOS devices. As previously noticed by one of the present authors,³¹ the conductance change $\delta\sigma/\sigma$ due to the band structure is much more important in MOS than in MIM systems. For the MIM systems, because of the flat band structure, the conductance change is very small and roughly constant with bias; whereas for the MOS systems, on the contrary, there is a larger band bending structure and the conductance change is strongly dependent on the bias voltage. The typical change in conductance due to onset of a tunneling channel via the phonons is about 1% (more accurately 0.4% found by Klein and Leger²⁹) in MIM junction. In contrary, the conductance change is strongly enhanced (about 12%) in the MOS junction due to the very weak conductance at this small bias. Consequently, as the MOS tunneling junction conductance σ increases with increasing bias, it becomes more and more difficult to detect IETS peaks at high energy levels. For this reason, we have focused our attention on the phonon peaks at low energy in such silicon-based junctions.

B. Phonons of the silicon substrate

The IET phonon spectrum of the Al-SiO₂-Si (*n*⁺) in the bias range of 30–70 meV and the structure relative to lattice vibrations of the crystalline silicon are clearly visible for both the (100) and (111) silicon orientations. These two spectra are shown, Fig. 6, in the extended range of 20–140 meV. First, we can check that the intensity of peaks due to silicon phonons in the expected bias range (30–70 meV) are clearly stronger than other peaks at higher bias (70–140 meV). Second, the two phonon spectra are not identical. The deconvolutions of these spectra were performed with the use of a special data analysis software (PEAKFIT).³²

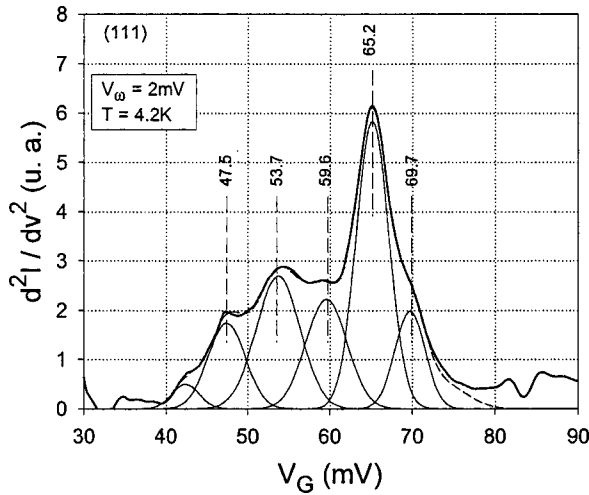


FIG. 7. Deconvolution of silicon phonon modes for an Al-SiO₂-Si (*n*⁺) doped with phosphorus [silicon orientation (111)].

1. (111) silicon orientation

The IET spectrum of the (111) silicon phonon was already investigated in the previous paper.²² These first results were rather involved and inaccurate due to a too large modulation ($V_\omega = 5$ mV). We have seen in Part II that the optimum voltage modulation at $T = 4.2$ K is 1.6 mV. In the present work, the spectrum may be deconvoluted as shown in Fig. 7 in essentially five peaks: the most intense at exactly 65.3 meV (527 cm^{-1}) is due to an interaction of the tunneling electron and the $k=0$ longitudinal optical phonons of silicon³³ (Γ point), as is seen in metal-insulator-semiconductor tunnel junctions fabricated with *p*-type silicon, though the conduction mechanism is not the same. In its pioneering work on *p*-type silicon, Wolf^{34,35} has reported this main peak at 64.9 meV.

The second peak at 47.5 meV (383 cm^{-1}) and the third at 53.7 meV (434 cm^{-1}) are assigned, respectively, to the longitudinal acoustical (LA) and longitudinal optical (LO) phonons of a wave vector k at the Brillouin zone boundary in the (111) direction (L point). In addition, there is a fourth mode, not detected in our previous work²² because it was embedded in the whole band vibration. This small peak appearing at 59.6 meV (481 cm^{-1}) may be assigned to the transversal optical (TO) phonon mode in the (100) direction (X point). It may appear surprising to detect a (100) silicon mode phonon on the (111) silicon interface corresponding to the no-specular transmission of electronic wave vector. This is an indication that the interaction of tunneling electrons with the electrode phonon may occur farther in the electrode lattice. The energies of these four peaks are in good agreement with the measurements using neutron scattering³⁶ and basic text book.³⁷ A summary of these assignments is given in Table I.

2. (100) silicon orientation

If, in the (111) directions, the relative conduction band minima occur at the Brillouin zone boundaries, the situation is a little more complicated in the (100) direction. In that case, the conduction band has six symmetry-related minima

TABLE I. Characteristic energy of silicon phonons for the (111) orientation.

Γ	L point		X point
TO mode	LA mode	LO mode	TO mode
65.2 mV	47.5 mV	53.7 mV	59.6 mV

at points about 85% of the way to the zone boundary.³⁸ Strong electron-phonon interactions can be expected in these bulk silicon band conduction minima. The IET phonon spectrum for the (100) silicon orientation has been deconvoluted after removing the elastic tunneling background [Fig. 8(a)]. Six peaks appear clearly. This figure must be brought closer together with the one in the paper by Lye and co-workers.³⁹ Their deconvolution (Fig. 2 in Ref. 39) is very near to our Fig. 8(a) and leads to six separate modes. The most intense mode located at 60.1 meV (484 cm^{-1}) (59.4 meV in Ref. 39) is due to the TO phonon mode associated with conduction band minima in the (100) direction. This strong mode was also reported at 56.6 meV (457 cm^{-1}) by Kulda *et al.*⁴⁰ Infrared absorption measurement performed by Balkanski and Nazarewicz⁴¹ identifies this mode at 60.3 meV (486 cm^{-1}). Again, the comparison with neutron scattering data shows a good agreement [within the error bars of the neutron data, typically a few meV (Ref. 40)]. The two peaks on Fig. 8(a),

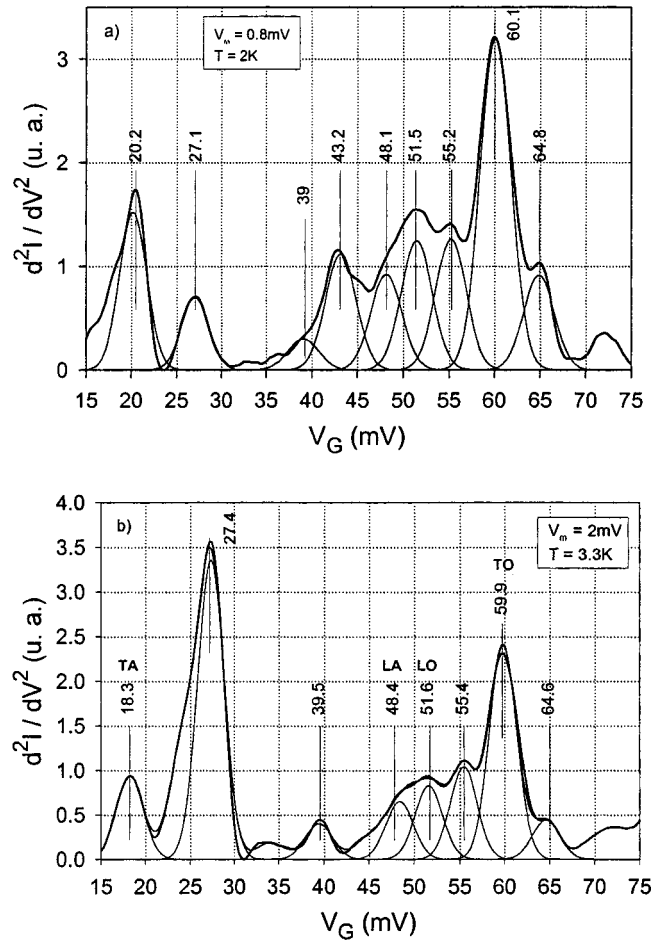


FIG. 8. Deconvolution of silicon phonon modes [silicon orientation (100)] for an Al-SiO₂-Si (*n*⁺) (a) doped with phosphorus, (b) doped with arsenic.

TABLE II. Characteristic energy (in meV) of silicon phonons for the (100) orientation.

Author	This work		Pepper ^a		Lye ^b	Bencuya ^c	
	Si:P	Si:As	Si:P	Si:As	Si:P	Si:P	Asche ^d
Δ_5 TA mode in X point	20.2	18.3	17.9	18.8	19	18	18.4
Σ_3 acoustic phonon to K point	27.1	27.4	31.5	30.5	36.8		
Σ'_1 or Δ_1 LA mode in X point	43.2	48.4	48.5	48.5	43.6	48.0	46.3
Δ'_2 LO mode toward X point	51.5	51.6	51.8	51.0	53.6	56.2	54.5
Σ_1 or Σ_2 TO mode toward X point	60.1	59.6	60.4	60.0	59.4	59.1	57.8

^aReference 42.^bReference 18.^cReference 17.^dReference 43.

flanking the main silicon mode and situated at 64.8 meV and 55.2 meV (63.4 meV and 53.6 meV in Ref. 39) are assigned to two low energy phonon modes of SiO₂. The main vibration modes of SiO₂ are at higher energy (130–170 meV) (see Sec. IV). The fourth peak located at 43.2 meV (348.5 cm⁻¹) (43.6 meV in Ref. 40, but 46.3 meV in Table I of Ref. 30) is attributed to Σ_1 or δ_1 LA phonon mode. The low energy isolated peak occurring at 20.2 meV (163 cm⁻¹) is ascribed to a δ_5 transversal acoustical (TA) mode towards X point at the conduction band minimum. Finally, always towards X point, there is a phonon mode at 51.5 meV (415 cm⁻¹) which is assigned to the δ'_2 LO mode. We cannot assign the peak occurring at 48.1 meV (388 cm⁻¹). The mode at 27.1 meV (218 cm⁻¹) may be attributed to a TA phonon at point with Σ_3 symmetry. This last mode [the only one which is not in the (100) direction], according to the Pepper's work,⁴² is small for phosphorous doping, and very strong for arsenic doping as we can see in Fig. 8(b). The assignments of all these phonon modes, and their energy position measurements compared with literature data, are summarized in Table II.

IV. IETS SPECTRUM OF SiO₂ PHONONS

For very thin SiO₂ layers (1–5 nm) used in microelectronic devices, ballistic transport is observed.^{44,45} From these ballistic transport studies, mean free paths in the range from 7 to 15 Å are deduced. The oxide thickness is barely larger

than this range. Then, evolutions and changes in the IETS spectrum of SiO₂ phonons are expected under electrical stresses due to changes in the structural organization (defect, charge trapping, ...) of the SiO₂. An IETS spectrum obtained at 4 K on an Al-SiO₂-Si (100) (n^+) sample is shown in Fig. 9, focusing on the range of silicon dioxide phonons. It is compared with previous spectra obtained for (111) silicon tunnel junction (Fig. 10).⁴⁶ The deconvolution and analysis for the (111) Si device was already presented in the preceding paper.⁴⁶ The deconvolution of the SiO₂ vibration band for the Si(100) junction is shown in Fig. 9. The peaks exhibit the same energy position as those for the Si(111) device reported in our previous paper.²² The main discrepancy between the two orientations comes from the mode magnitude. For instance, the asymmetric stretch TO4 mode assigned theoretically at 148.8 meV (1200 cm⁻¹) according to Kirk's work⁴⁷ appears as a strong peak at 149.0 meV (1202 cm⁻¹) in the Si(111) junction, but it appears as a weak peak in the (100) orientation, slightly shifted at 149.9 meV (1210 cm⁻¹). It is curious that the TO4 and LO4 modes have the same intensity in the SiO₂ thermally grown on Si(111) and different intensities on Si(100). Following the first theoretical investigation⁴⁸ of vibrational mode intensities in IETS, the ratio of intensities should be different for different orientations of the molecular dipoles in the tunnel oxide barrier. We think that the SiO₄ tetrahedrons may be stacked in different

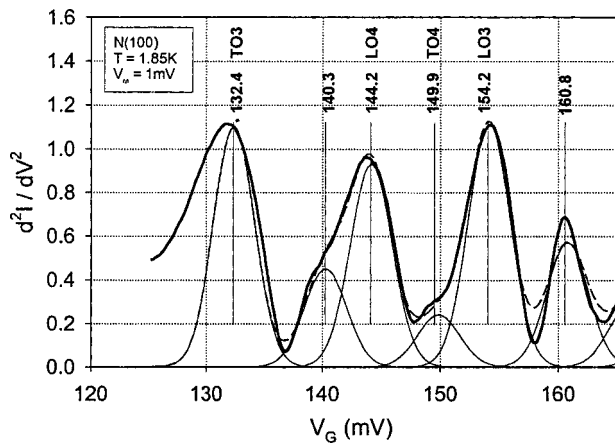
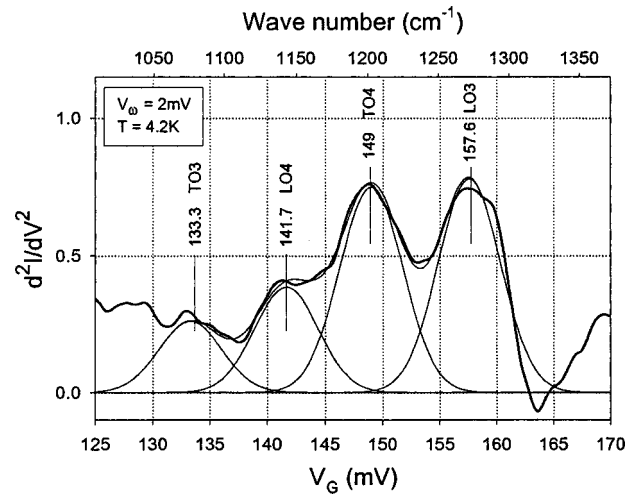
FIG. 9. Deconvolution in separated modes of SiO₂ vibration band on (100) silicon orientation for an Al-SiO₂-Si (n^+).FIG. 10. Deconvolution in separated modes of SiO₂ vibration band on (111) silicon orientation for an Al-SiO₂-Si (n^+).

TABLE III. Characteristics energy of SiO₂ phonons.

		Silicon orientation			
		(100)		(111)	
Authors		Kirk ^a	Lye ^b	This work	Previous work ^c
Modes					
Rocking	TO1	56.7 mV		55.2 mV	
	LO1	62.8 mV		64.8 mV	
Asymmetrical stretching	TO3	133.4 mV	131.6 mV	132.4 mV	133.3 mV
	LO4	143.8 mV	143.3 mV	144.2 mV	141.7 mV
	TO4	148.8 mV	147.4 mV	149.9 mV	149.0 mV
	LO3	155.7 mV	154.8 mV	154.2 mV	157.6 mV

^aReference 47.
^bReference 18.
^cReference 22.

ways depending on the silicon orientation. The other assignments of the detected vibration modes are recapitulated in Table III and compared with literature. Our analysis is consistent with the first deconvolution published by Lye *et al.*³⁹ (see Table III for comparison). It could be emphasized that the assignments of the SiO₂ phonon modes are identical on both silicon orientations (100) (Ref. 39) and (111).²² The conductance change ratio $\Delta\sigma/\sigma$ due to inelastic SiO₂ phonon effect is very weak (0.42%–0.8%), making detection of IET peaks difficult, especially for the case of Si(100) tunnel junction.

V. EFFECTS OF ELECTRICAL STRESSES ON SiO₂ PHONON IET SPECTRUM

Gate oxide degradations induced by high electrical stresses are intensely investigated in microelectronics.^{49,50} Defects, traps, and positive or negative oxide charges are usually detected after having applied a constant voltage(CVS) or current stress.^{51–53} Any modification of the SiO₂ atomic structure (bond breaking, bond deformation, trapped charges, ...) is supposed to influence the vibrational modes of the SiO₂ film. Thus, IETS could be an interesting technique to probe the reliability of ultrathin gate electric (<3 nm), a thickness range where other standard methods (C-V, I-V, charge pumping, ...) become more and more difficult to use and to interpret. To prove the influence of IETS as a tool for reliability study, we have performed a series of IETS measurements after applying several and different electrical stresses. For an Al-SiO₂-Si (n⁺), we have applied the following sequence of electrical stresses on the same sample at liquid helium temperature and measured the IET spectrum (Si phonon range only) after each stress.

- (1) CVS at V_g=+0.8 V (or F=4 MV/cm) during 10 min (curve 2 in Fig. 11).
- (2) CVS at V_g=-2.0 V (or F=-10 MV/cm) during 10 min (curve 3).
- (3) Warm-up the sample to room temperature for 24 h (annealing) (curve 4).

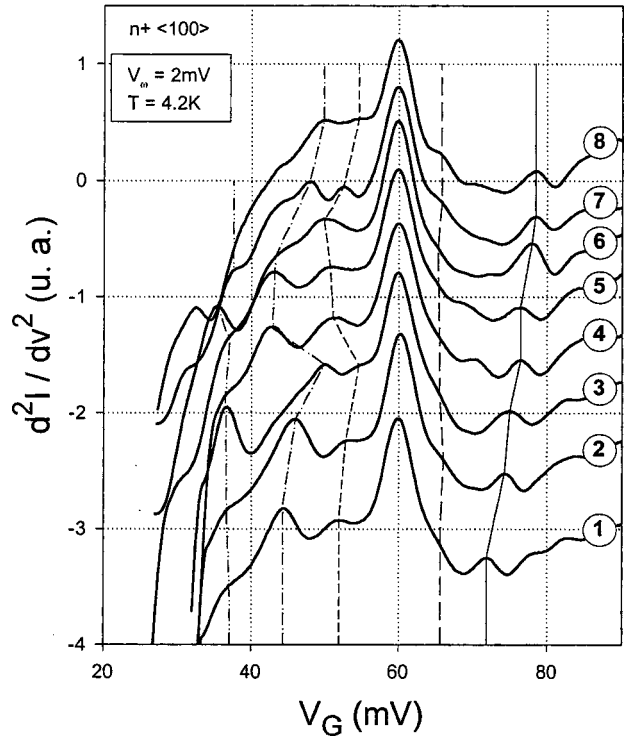


FIG. 11. IET spectra of phonon modes after and before electrical stresses. The curves labeled are: 1, initial; 2, after CVS, +0.8 V, 10 min; 3, after CVS -2 V, 10 min; 4, after warm-up, 24 h; 5, 19 h later; 6, after CVS, +2 V, 10 min; 7, after CVS, +2.5 V, 5 min; 8, after CVS, +3 V, 5 min. The stress and measurements shown are on the same sample with the electrical stress being cumulative.

- (4) 19 h later at liquid helium temperature (curve 5).
- (5) CVS at V_g=+2.0 V (or F=+10 MV/cm) during 10 min (curve 6).
- (6) CVS at V_g=+2.5 V (or F=+12.5 MV/cm) during 5 min (curve 7).
- (7) CVS at V_g=+3.0 V (or F=+15 MV/cm) during 5 min (curve 8).

The IETS spectra taken after each electrical stress are shown in Fig. 11, and the change in energy of the five main phonon modes, measured from the IET spectrum of the Fig. 11, are shown in Fig. 12. First, we note that the most impor-

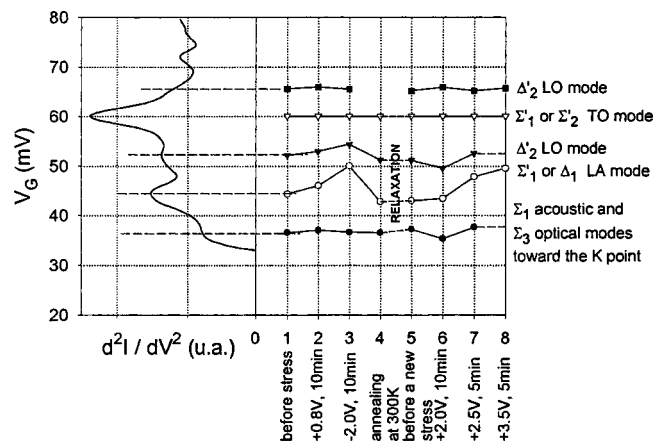


FIG. 12. Modification of phonon mode energy positions induced by electrical stresses.

tant mode located at 60 meV remains unaffected. This lattice vibration excited by the electrons belonging to an ellipsoid of revolution³⁸ along a (100) cube axis corresponds, in the spectrum, to the smallest k wave vector, consequently to the largest wave length. We can understand that the Si-SiO₂ interface modification induced by the electrical stress is only altered in the first silicon monolayer. On the contrary, the two peaks located at 44.3 meV and 52.5 meV and assigned to the Σ_1 or Δ_1 LA mode and Δ'_2 LO mode are the most affected by this electrical stress sequence. Longitudinal lattice vibrations seem to be more affected at the silicon interface than transversal modes.

It is well known that electrical stresses can perturb the Si-SiO₂ interface, breaking some bonds or changing the bond length of the Si atoms with gate oxide SiO₂. Massoud⁵⁴ has emphasized the existence of one dipole moment of the Si-SiO₂ interface. According to this author, the charge transfer is not limited to the interface bond only; it also takes place in bonds beyond the interface both in the silicon substrate and the silicon dioxide layer. The interface dipole polarity is located along the silicon atom arrays, and the applied electrical stresses may change the bond length of the Si atoms with gate oxide, affecting the longitudinal force constant β_L and slightly modifying the frequency $\omega = \sqrt{\beta_L/m_{\text{Si}}}$ where m_{Si} is the silicon atom mass. It would be necessary to perform EXAFS, SEXAFS, and ELFS techniques in order to confirm or invalidate this explanation.

This effect is not analyzed in more detail here, further works are in progress. The second feature is the reversibility of the degradation probed by IETS. After a 24 h warmup at room temperature, previously shifted peaks have actually gone back to lower voltage than initial curve and the IET spectrum has recovered almost its initial characteristic. Subsequent CVS (increasing stress field) shows again the significant energy shift of the Σ'_1 or Δ_1 LA mode (while the Δ'_2 LO mode seems less affected than during the first CVS sequence). The peak at 70 meV is also affected by electrical stresses. After Tsui and Dunkelberger⁵⁵ and Vratny *et al.*,⁵⁶ this peak can be attributed to vibrational mode of silicon oxide. These different shifts modify slightly the energy positions. We think that these modifications are due to fluctuations in the measurements, but, as we can see on the curves 4 and 5 in Fig. 12, 19 h separate these two measures and there are no shifts in energy positions.

We have only scanned the effects of stresses in the silicon phonon range. But Lye *et al.*¹⁸ have observed the modification of oxide vibrational modes' structures by electrical stresses. Some modifications appear in the magnitude of peaks for some modes. But no shift is detected in the energy positions.

These preliminary results show that IETS is a valuable tool to get structural information on damages induced by stress.

VI. CONCLUSION

In this paper, we have continued to investigate the application of tunneling spectroscopy to the silicon MOS devices. The properties of ultrathin insulators and their interfaces

with semiconductors and gate electrodes are always critical topics to the semiconductor microelectronics industry. In the past, IETS was demonstrated as an *in situ* nondestructive spectroscopy technique, for MIM tunnel junctions. Nowadays, in state-of-the-art MOS devices, the gate oxide has reached thickness below 3 nm so that tunnel phenomena take place. Thus, the IETS technique can now be applied in these devices. We have analyzed the phonon IET spectrum of each of the three parts constituting the tunnel silicon MOS junction.

(a) Aluminium gate: Phonons of Al gate were compared to the MIM results and the aluminium qualified as granular.

(b) SiO₂ tunnel barrier: Phonons of SiO₂ barrier were observed for both (111) and (100) silicon substrates. The analysis of the vibrational modes of SiO₂ grown on (111) silicon is very near to the analysis by Lye *et al.*³⁹ of SiO₂ grown on (100) orientation. The main difference between the phonon spectra for SiO₂ grown on (111) or (100) Si comes from the respective amplitudes of the peaks. This may be ascribed to local change in the orientation of the molecular dipoles in these oxides.

(c) Silicon substrate: The IET lattice vibration spectra of silicon substrate were obtained for both (100) and (111) orientations. Phonon vibration bands were deconvoluted in separate modes and these modes were assigned in energy in good agreement with literature.

An interesting energy shift induced by electrical stresses is reported and in the most part explained. This may constitute a new interface characterization in MOS devices. We show that IETS can reveal changes in the Si-SiO₂ interface induced by electrical stresses. The Si longitudinal phonon peaks are shifted by constant voltage stress (performed at 4.2 K), while transversal phonon modes remain unaffected. Further studies are in progress to deeply analyze these features.

ACKNOWLEDGMENTS

The authors thank W.K. Lye for fruitful discussions. This work was supported by French RMNT (Micro Nano Technology Network) and was performed in the mainframe of the ULTIMOX project, in collaboration with the following companies and laboratories: CEA-LETI (Grenoble), STMicroelectronics (Crolles), LPM (INSA de Lyon), IMEP (ENSERG Grenoble), L2MP (ISEM Toulon).

¹G. Ghibaudo, P. Priess, S. Bruyere, B. De Salvo, C. Jahan, A. Scarpa, G. Pananakakis, and E. Vincent, *Microelectron. Eng.* **49**, 41 (1999).

²S.-I Takagi, N. Yasuda, and A. Toriumi, *IEEE Trans. Electron Devices* **46**, 335 (1999).

³S.-I Takagi, N. Yasuda, and A. Toriumi, *IEEE Trans. Electron Devices* **46**, 348 (1999).

⁴B. F. Lewis, M. Mosesman, and W. H. Weinberg, *Surf. Sci.* **41**, 142 (1974).

⁵S. Gauthier, S. De Cheveigne, G. Salace, J. Klein, and M. Belin, *Surf. Sci.* **155**, 31 (1985).

⁶J. Klein, A. Leger, M. Belin, D. Defourneau, and M. J. L. Sangster, *Phys. Rev. B* **7**, 2336 (1973).

⁷M. G. Simonsen and R. V. Coleman, *Phys. Rev. B* **8**, 5875 (1973).

⁸P. K. Hansma and R. V. Coleman, *Science* **134**, 1369 (1974).

⁹N. M. D. Brown, R. B. Floyd, and D. G. Walmsley, *J. Chem. Soc., Faraday Trans. 2* **75**, 32 (1979).

¹⁰*Tunneling Spectroscopy*, edited by P. K. Hansma (Plenum, New York,

- 1982).
- ¹¹R. C. Jaklevic and J. Lambe, *Phys. Rev. Lett.* **18**, 1139 (1966).
- ¹²K. Kudo, C. Okazaki, S. Kuniyoshi, and K. Tanaka, *Jpn. J. Appl. Phys., Part 1* **30**, 1452 (1991).
- ¹³M. Wada, T. Kubota, and M. Iwamoto, *Jpn. J. Appl. Phys., Part 1* **32**, 3868 (1993).
- ¹⁴J. L. Brousseau, S. Vidon, and R. M. Leblanc, *J. Chem. Phys.* **108**, 7391 (1998).
- ¹⁵J. Murai, Y. Ando, M. Kamijo, H. Kubota, and T. Miyazaki, *Jpn. J. Appl. Phys., Part 1* **38**, 1106 (1999).
- ¹⁶R. J. M. Van De Veerdonk, J. S. Moodera, and W. J. M. De Jonge, *J. Magn. Magn. Mater.* **152**, 198 (1999).
- ¹⁷I. Bencuya, Ph.D. Thesis U.M.I Dissertation Information Service, 1984.
- ¹⁸W. K. Lye, T. P. Ma, R. C. Barker, E. Hasegawa, Y. Hu, J. Khuene, and D. Frystak, *International Conference on Characterization and Metrology for U.L.S.I. Technology, 1998*, edited by D. G. Seiler, A. C. Diebold, W. M. Bullis, T. J. Shaffner, R. McDonald, and E. J. Walters (American Institute of Physics, New York, 1988), p. 261.
- ¹⁹H. G. Busmann, S. Ewert, W. Sander, K. Seibert, P. Balk, and A. Steffen, *Z. Phys. B: Condens. Matter* **59** 439 (1985).
- ²⁰P. Balk, S. Ewert, S. Schmitz, and A. Steffen, *J. Appl. Phys.* **69**, 6510 (1991).
- ²¹S. Kuniyoshi, O. Suzuki, K. Kudo, and K. Tanaka, *Trans. Inst. Electr. Eng. Jpn., Part A* **116**, 80 (1996).
- ²²G. Salace, C. Petit, and D. Vuillaume, *J. Appl. Phys.* **91**, 5896 (2002).
- ²³C. Petit and G. Salace, *Rev. Sci. Instrum.* **74**, 4462 (2003).
- ²⁴H.-X. Shen and H.-C. Li, *Chin. Phys.* **2**, 232 (1982).
- ²⁵D. G. Walmsley, R. B. Floyd, and S. F. J. Read, *J. Phys. C* **11**, L107 (1978).
- ²⁶K. W. Hipps and U. Mazur, in *Handbook of Vibrational Spectroscopy*, edited by J. M. Chalmers and P. R. Griffiths (Wiley, Chichester, 2002).
- ²⁷L. J. Lauhon and W. Ho, *Rev. Sci. Instrum.* **72**, 216 (2001).
- ²⁸J. Klein, Ph.D. Thesis, University of Paris, 1969.
- ²⁹J. Klein and A. Leger, *Phys. Lett.* **28A**, 134 (1968).
- ³⁰J. P. Carbotte and R. C. Dynes, *Phys. Lett.* **25A**, 685 (1967).
- ³¹G. Salace and J. M. Patat, *Thin Solid Films* **207**, 213 (1992).
- ³²PEAKFIT, SPSS Inc., Chicago, IL 60611.
- ³³L. B. Schein and W. C. Compton, *Appl. Phys. Lett.* **17**, 236 (1970).
- ³⁴E. L. Wolf, *Phys. Rev. Lett.* **20**, 204 (1968).
- ³⁵D. E. Cullen, E. L. Wolf, and W. D. Compton, *Phys. Rev. B* **2**, 3157 (1970).
- ³⁶B. N. Brockhouse, *Phys. Rev. Lett.* **2**, 256 (1959).
- ³⁷C. Kittel, *Physique de l'état solide*, 7th ed. (Dunod, Paris, 1998).
- ³⁸N. W. Ashcroft and N. D. Mermin, *Solid State Physics*, (Sanders College Publishing, Philadelphia, 1976), p. 569.
- ³⁹W. K. Lye, E. Hasegawa, T. P. Ma, R. C. Barker, Y. Hu, J. Kuehne, and D. Frystak, *Appl. Phys. Lett.* **71**, 2523 (1997).
- ⁴⁰J. Kulda, D. Strauch, P. Davoine, and Y. Ishii, *Phys. Rev. B* **50**, 13347 (1994).
- ⁴¹M. Balkanski and W. Nazarewicz, *J. Phys. Chem. Solids* **23**, 573 (1961).
- ⁴²M. Pepper, *J. Phys. C* **13**, 709 (1980).
- ⁴³M. Ashe and O. G. Sarbei, *Phys. Status Solidi B* **103**, 11 (1981).
- ⁴⁴D. J. Di Maria, M. V. Fischetti, J. Batey, L. Dori, E. Tierney, and J. Stasiak, *Phys. Rev. Lett.* **57**, 3213 (1986).
- ⁴⁵M. V. Fischetti, D. J. Dimaria, L. Dori, J. Batey, E. Tierney, and J. Stasiak, *Phys. Rev. B* **35**, 4404 (1987).
- ⁴⁶C. Petit, G. Salace, and D. Vuillaume, *Solid-State Electron.* **47**, 1663 (2003).
- ⁴⁷C. T. Kirk, *Phys. Rev. B* **38**, 1255 (1988).
- ⁴⁸J. Kirtley, D. J. Scalapino, and P. K. Hansma, *Phys. Rev. B* **14**, 3177 (1976).
- ⁴⁹J. H. Stathis, *IBM J. Res. Dev.* **46**, 265 (2002).
- ⁵⁰A. Meinertzhagen, C. Petit, D. Zander, O. Simonetti, T. Maurel, and M. Jourdain, *J. Appl. Phys.* **91**, 2123 (2002).
- ⁵¹D. J. Dimaria and W. J. Stasiak, *J. Appl. Phys.* **65**, 2342 (1989).
- ⁵²M. V. Fischetti, *J. Appl. Phys.* **57**, 2860 (1985).
- ⁵³D. J. Dimaria, E. Cartier, and D. Arnold, *J. Appl. Phys.* **73**, 3367 (1993).
- ⁵⁴H. Z. Massoud, *J. Appl. Phys.* **63**, 2000 (1988).
- ⁵⁵D. Tsui and L. N. Dunkelberger, *Appl. Phys. Lett.* **18**, 200 (1971).
- ⁵⁶F. Vratny, M. Dilling, F. Gugliotta, and C. N. R. Rao, *J. Sci. Ind. Res.* **20B**, 590 (1961).